BILINGUAL PUBLISHING CO.
Pioneer of Global Academics Since 1984

Journal of Geological Research
http://ojs.bilpublishing.com/index.php/jgr-a

ARTICLE

Comparison of U-spatial Statistics Method with Classical Statistics Results in the Determination of Geochemical Anomalies of Epithermal Gold in Khoshnameh Area, Hashtjin, Iran

Mirmahdi Seyedrahimi-Niaraq*

Faculty of Engineering, University of Mohaghegh Ardabili, Ardabil, Iran.

ARTICLE INFO

Article history
Received: 04 March 2021
Accepted: 29 March 2021
Published Online: 20 April 2021

Keywords:
Geochemical exploration
U-Spatial statistics method
Anomalous area
Epithermal gold

ABSTRACT

In this study, methods based on the distribution model (with and without personal opinion) were used for the separation of anomalous zones, which include two different methods of U-spatial statistics and mean plus values of standard deviation ($\overline{X} + nS$). The primary purpose is to compare the results of these methods with each other. To increase the accuracy of comparison, regional geochemical data were used where occurrences and mineralization zones of epithermal gold have been introduced. The study area is part of the Hashtjin geological map, which is structurally part of the folded and thrust belt and part of the Alborz Tertiary magmatic complex. Samples were taken from secondary lithogeochemical environments. Au element data concerning epithermal gold reserves were used to investigate the efficacy of these two methods. In the U- spatial statistics method, and criteria were used to determine the threshold, and in the method, the element enrichment index of the region rock units was obtained with grouping these units. The anomalous areas were identified by, and criteria. Comparison of methods was made considering the position of discovered occurrences and the occurrences obtained from these methods, the flexibility of the methods in separating the anomalous zones, and the two-dimensional spatial correlation of the three elements As, Pb, and Ag with Au element. The ability of two methods to identify potential areas is acceptable. Among these methods, it seems the method with criteria has a high degree of flexibility in separating anomalous regions in the case of epithermal type gold deposits.

1. Introduction

Geochemical haloes are areas around the ore deposit where the concentration of elements with ore solutions is chemically higher than usual, but the concentration of elements may not have reached the level of economic mineralization in some deposits [1-8]. A characteristic of these haloes is their much broader expansion than the deposit, which makes it easier to explore mineral deposits. These haloes extend like the pod around the deposit. The shape and extent of expansion of these haloes depend on several factors, such as the form and amount of mineral deposit, the content of mineral reservoir, and the kind of host rock[9-18].

**Corresponding Author:*
Mirmahdi Seyedrahimi-Niaraq,
Faculty of Engineering, University of Mohaghegh Ardabili, Ardabil, Iran;
Email: m.seyedrahimi@uma.ac.ir

 DOI: https://doi.org/10.30564/jgr.v3i2.2935

The concentration threshold refers to a certain amount of concentration in geochemical exploration and projects, which based on that can separate geochemical anomalous (Values higher than threshold concentration) and background (Values smaller than threshold concentration) from each other [1, 2]. In the concept of the anomaly, Rose et al. [19] stated that the element concentration threshold is an indicator in which the concentrations higher than that is an anomaly. In the simplest case, it can be said that the threshold is the upper limit of the background so that the values above this limit are the anomaly, and the lower values are the background. However, in most cases, two or more threshold values may be detected [20-25]. In geochemical investigations, anomalous values can be related to mineralized rocks. Therefore, the threshold value is a crucial exploration guideline for selecting anomalous samples, or in other words, where the chance of discovering the mineral deposit is very high [1]. Part of the anomaly population is related to these haloes and another part to the ore deposit [26]. Therefore, in the first stage of geochemical exploration should be identified the anomalous values and then the anomalous areas should be prioritized.

Different methods have been used for the separation and detection of anomalous zones from the background. These methods can be divided into three distinct groups. The first group is based on the statistical parameters of the distribution (such as the mean plus twice the standard deviation method), the second group, which is more complicated than the previous one, considers the frequency distribution of the element concentration (for example, probability graphs and gap statistic methods). The last group considers the location of the sampling points and their spatial relation in estimating anomalous zones (such as U-spatial statistics and fractal and multifractal method, and machine learning-based algorithms) [27-37].

All of these methods follow from a general-purpose, as illustrated in Figure 1. This Figure represents the distribution frequency of concentration values (these values may be raw values or values estimated by moving averages or kriging). Anomaly (A) and background (B) are two distinct populations that differ in element content and spatial properties. These methods aim is to define a threshold so that element values can classify samples. Samples with values higher than z are the anomaly population, and values smaller than z are the background population. If z_1 is the lower limit of the anomaly and z_2 is the upper limit of the background, samples with a value less than z_1 can be considered background and more than z_2 as an anomaly (Figure 1). If two populations A and B overlap, then there are two different values z_A and z_B $z_{A<}$ z_B), and samples are certainly not classified between these two values since these samples can belong to both the anomaly and background populations [38].

As the purpose of a regional geochemical exploration project is to introduce potential areas for further study, anomaly zones should be carefully identified. Different methods have been proposed for this purpose. In these methods, two types of errors are always associated with the classification. These two types of errors are inversely correlated, the first (e_1) occurs when the sample of background population is not counted with the background value, and the second (e_2) occurs when the sample of the anomaly population is counted with the background value. These two types of errors are also inverted, meaning that if one type of error decreases with the threshold change, the other increases. In some cases, minimizing one of the errors has the best result, but in other cases, it is better to minimize the total error [38].

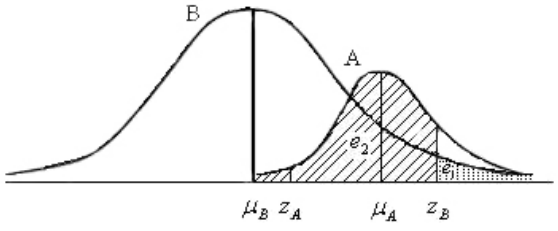

Figure 1. Density function of a geochemical variable showing two populations [7]: (A) anomaly with mean μ_A; (B) background with mean μ_B. z_A = lower limit of an anomaly; z_B = upper limit of background. e_1 and e_2 = errors of type 1 and 2 with z_B as a threshold.

In this research, a basic map for measuring the efficiency of methods is provided. This map is the summary of the geological map, in which the results of regional and local exploration studies, including the mineralized area, were fitted on that. Then two methods of U-spatial statistics and are applied to data. The results of these methods will be to determine the threshold values and map of the anomalous areas. For evaluating the methods, the results are compared with the basic map.

2. Geology and Tectonic Setting

The study area is part of the Hashtjin geological quadrangle, which is located 20 km south of Khalkhal in the following geographical coordinates (Figure 2):

N37° 30’ 00.0” E48° 16’ 22.0”
N37° 30’ 00.0” E48° 27’ 18.0”
N37° 25’ 24.0” E48° 27’ 18.0”
N37° 25’ 24.0” E48° 16’ 22.0”

The geological map of the study area is shown in Figure 3(a), which shows the wide variety of these rock units in the region. The abbreviations of the rock units are de-

DOI: https://doi.org/10.30564/jgr.v3i2.2935

scribed in Table 1.

The oldest rock units in the study area are Paleocen' limestones, which locate adjacent to younger units in the form of fault (thrust). It is a sandy limestone or sandy biomicrite (Pgz) type of impure carbonate rocks. The main constituents of this unit are micrites and microsparites, which form the rocks. The most massive outcrop of the geological units in the area is identified by the composition of undisturbed basaltic volcanic rocks (E^{v1}) (TOZ 2003). These units have an almost northwest-southeast trend and mainly have andesitic to middle basaltic lavas and sometimes agglomerates with the same basic composition in the region. Between these two units, rocks with rhyolite to rhyodacite composition (OL^{v1}, P_t) and trachy basalt to trachyandesite (OL^{v2}) are penetrated. The most gold mineralization has occurred in these units. These units have appeared with smooth and rocky morphology in the area, respectively (Figure 4).

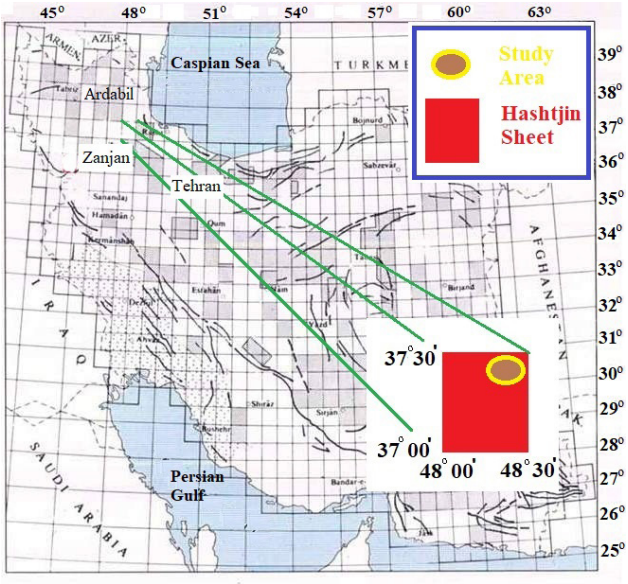

Figure 2. The geographical location of Hashtjin sheet (1:100000) and study area [7].

Tofogenic marls and acidic pyroclastics (E^m) are interlayers embedded within the unblocked E^{v1} basaltic volcanic rock unit. This rocky unit appears to belong to the lower parts of the E^{v1} unit.

Table 1. Legend of geological map of Khoshnameh area

Abbreviation	Description	Abbreviation	Description
Q^{al}	Recent alluvial-diluvial deposits, river beds	P^t	Acid vitric tuff, pumice
Qt_2	Younger terraces and alluvial deposits	E^{v1}	Undifferentiated basic volcanics
Qt_1	Old terraces	E^{ash}	Fin grain pyroclastics
PL^C	Grey conglomerate and sandstone	E^{da2}, E^{da1}	Andesite to dacite metavolcanic unit
$Ng2^m$	Red beds of marl, siltstone and sandstone	E^m	Mega porphyritic (Basaltic) andesite
OL^{v2}	Brown weathered trachybasalt and trachyandesite		
		Pg_z	Well bedded dark colored, spray limestone
OL^{v1}	Rhyolite, rhyodacite and volcaniclastic flow deposits		

 DOI: https://doi.org/10.30564/jgr.v3i2.2935

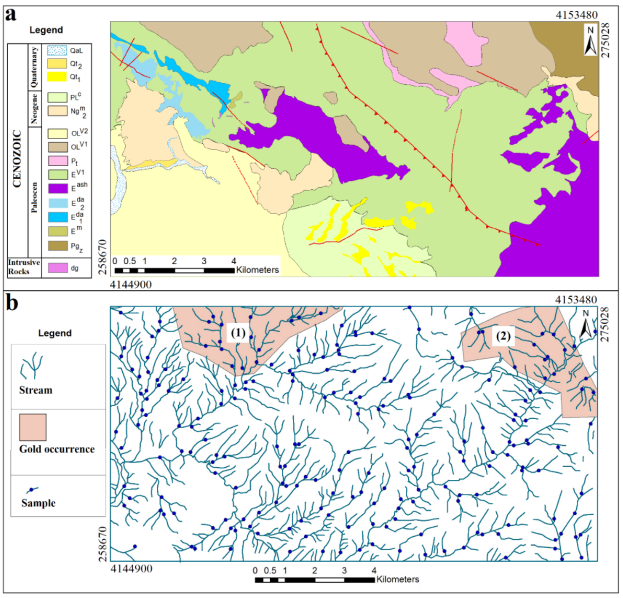

Figure 3. (a) Geological map of the study area in scale 1:20000 [40]. (b) Map of the position of the gold occurrences on the stream map; 1) The western limit of Khoshnameh, 2: Eastern and northeast limit of Beyraq.

The composition of this unit varies from tuff's marls to acidic pyroclastics, and its color changes from light gray to dark gray. Due to the nature of this unit, several landslides have occurred in some parts. The boundary of this unit is the fault at the main outlet in several directions. Andesite to dacite volcanic units (E^{da2}, E^{da1}) are exposed as acidic volcanic strata up to the middle in the northwestern parts of the area and around an anticline. The slope of these volcanic layers is different on both limbs of the anticline. In terms of field characteristics, this unit has an initial purple to pale pink color that has changed from milky to white due to alteration.

Field evidence shows a crystalline flow tuff to acidic lava that kaolinization and silicification can be seen in the stone. The lithological composition of the outcrops varies from andesite to dacite. From the structural point of view, the Hashtjin sheet is part of the folded and overthrust belt and part of the Alborz tertiary magmatic assemblage. Therefore, the rock units have different properties in this sheet. The study area is tectonically affected by two structural climates. The first includes the folded and overthrust belt of the western Alborz, located on the central Alborz magmatic units. The tectonic stresses from the northeast-southwest overthrust have caused the units to deform as these units follow a north-south-eastward trend, approximately [41].

3. Geochemical Data and Selection of Elements for the Study

Geochemical samples of stream sediment were collected in 215 samples. Because the streams and sediments were wet, all samples' volume was assumed to be 4 liters (depending on the sample size). The samples were dried in the field camp and at room temperature, and then all of them were screened with 80 mesh. After drying and sifting (-80 mesh), the geochemical samples were transferred to the preparation workshop. Then the whole samples were powder under the size of 200 mesh (-200 mesh). 100 gr of each sample were sent to the Amdel laboratory in Australia, and the rest was archived.

Base metal and trace element samples were analyzed by the ICP-MS method and based on dissolution in four acids. For obtaining analytical gold data, were used from the FIRE ASSAY standard process. Analysis on 44 elements includes Ag, As, Au, B, Ba, Be, Bi, Co, Cr, Cu, Hg,

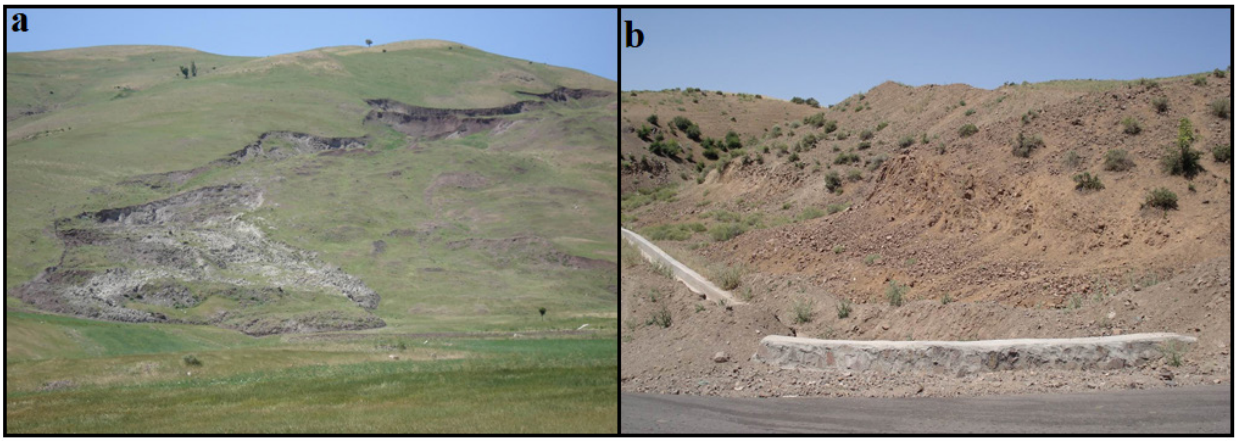

Figure 4. View of the outcrop of rhyolite, rhyodacite units (OL^{v1}) (a: smooth morphology) and trachy basalt, trachyandesite (OL^{v2}) (b: rocky morphology) [41].

DOI: https://doi.org/10.30564/jgr.v3i2.2935

Mn, Mo, Ni, Pb, Sb, Sn, Ti, V, W, Zn, Fe, Sr , Al, Sc, Ca, Li, P, Mg, K, Na, S, Zr, Cs, Nb, U, Th, Cd, Tt, Rb, Y, Ce, Tl, and La were performed. Among these elements, it was necessary to select a number of them based on their geochemical properties for research.

Since the gold element has smaller haloes and is also a little more challenging to study among many minerals, it is also one of the active projects in the exploration, so this element was selected to compare the threshold values determination methods. In order to further investigate the methods, some elements associated with gold were also selected. For this purpose, the correlation chart (Dendrogram) of the elements was prepared in the form of a dendrogram using IBM SPSS Statistics software, version 22. The correlation was performed using the Pearson method. The results are presented in Figure 5. The graph shows that the Au and Bi, Pb, As, Cd, Sb elements are versus the subgroup of Hg, Ag, Na, P, Mn, and Zn. Therefore, it deals with at least two general categories of the elements, and categories containing gold are selected here. As and Pb were also selected from among these elements for evaluating the methods' efficiency, because these elements are from the specificities of the epithermal deposits. The silver (Ag) element is not in the gold-containing subgroup (Figure 5) but is included in the epithermal type deposits with gold. Therefore, this element was also selected to investigate its dispersion further.

In statistical discussions, values that are significantly different from other values are called outlier values. These values are sometimes entered into the data due to experimental errors, such as analysis errors, but sometimes there are heterogeneity in the exploration data population [42]. Therefore, outlier values must be detected and subsequently corrected. In this project, outlier values are identified using the Q-Q plot, then reduced to their highest number that is not an outlier. Q-Q plot of the elements was presented in Figure 6. For example, the Pb element has two outlier values, and these two data are corrected to 3.56. By studying the Au element data, no outlier data were detected for this element.

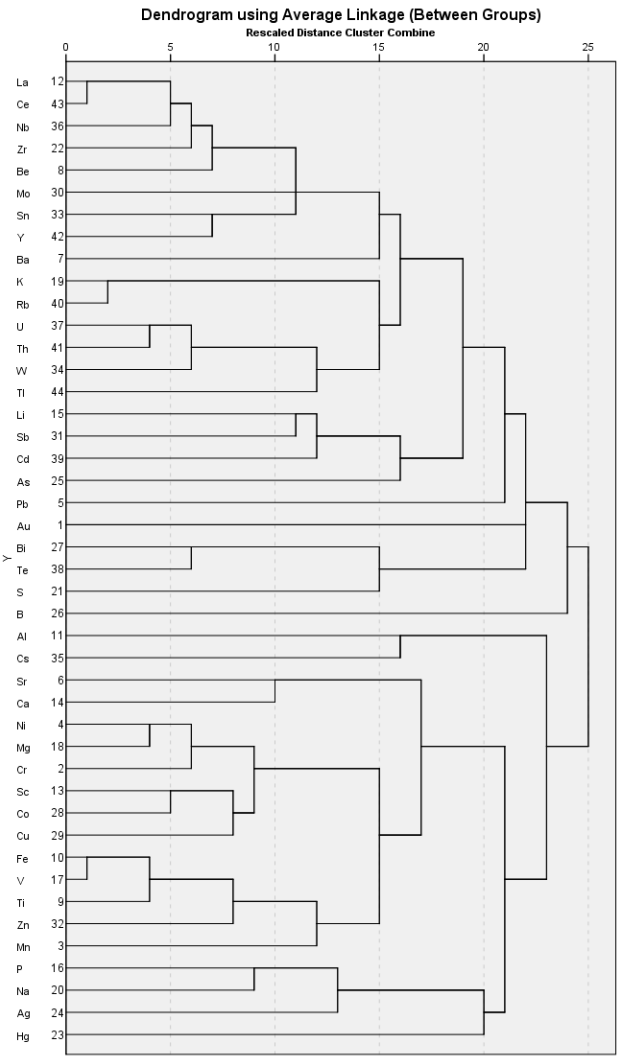

Figure 5. Correlation chart (Dendrogram) of the elements by the Pearson method.

The results of studies in the area led to the detection of the gold occurrences. Figure 3(b) shows a map of the position of the gold occurrences on the regional stream map. The location of the occurrences in the area is fitted on the obtained anomaly zones from the methods. This was done to compare the determination methods of the anomalous areas. The western limit of Khoshnameh, No. (1), is located in the north and northwestern part of the study area. The eastern and northeast limit of Beyraq, was marked with No. (2), is the other gold occurrence discovered in the area.

4. Methodology

Various anomaly separation methods, such as spatial statistics and mean plus values of standard deviation methods, were used to calculate the threshold value. The distribution variations were illustrated on a diagram or

 DOI: https://doi.org/10.30564/jgr.v3i2.2935

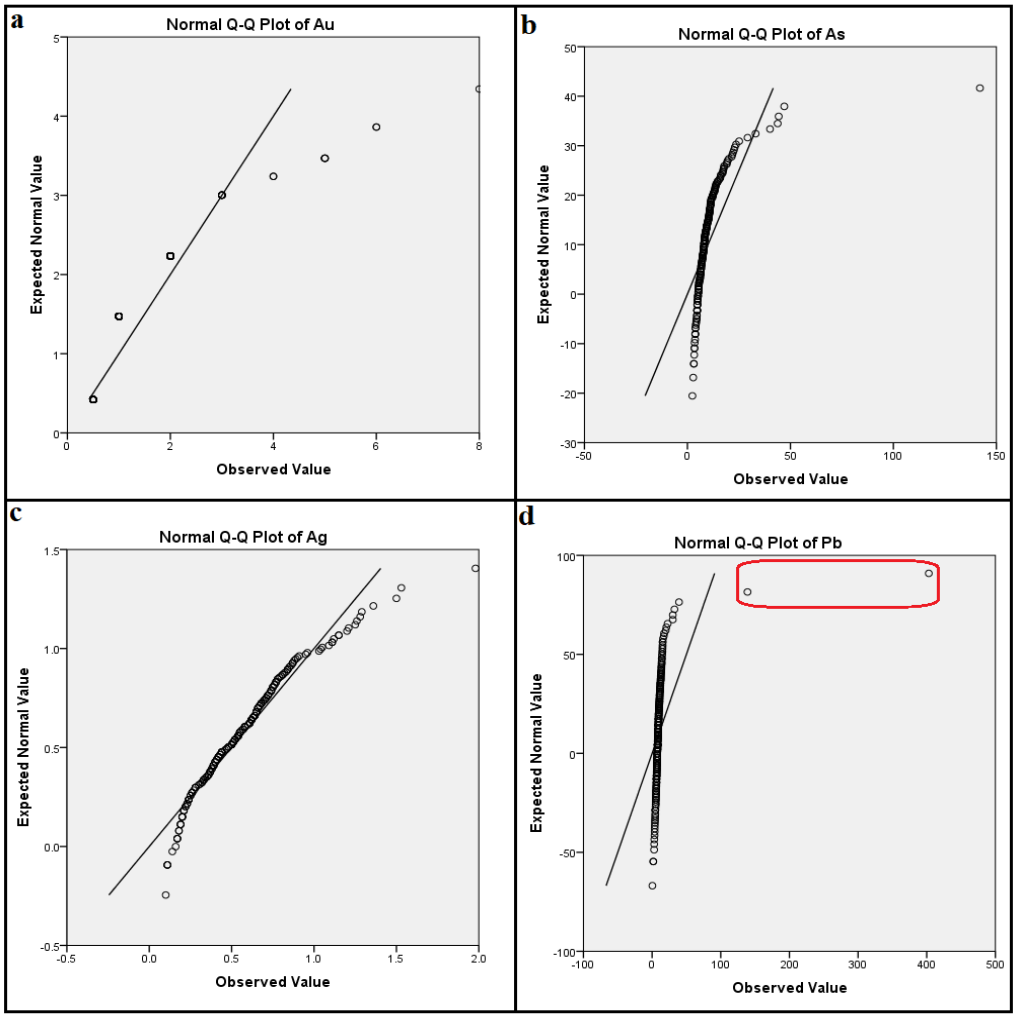

Figure 6. Q-Q plots of the elements Au(a), As(b), Ag(c) and Pb(d). Two outlier values are observed for the Pb element.

on histograms, and the anomalous areas were shown as isograd contour maps. Contour maps were provided by kriging interpolation technique with a suitable pixel size for raw or estimated data in the methods. The extension of secondary dispersion haloes was estimated by these maps. Subsequently, the results of different anomaly separation methods were compared based on geological information to determine these methods' accuracy.

4.1 U-spatial Statistics Method

The U-spatial statistics method is a moving average method that the dimensions of the window where the average is taken are changed at each particular point. Therefore, for each particular point, many U-statistic values are calculated using the points around inside the window. Thus, the spatial correlation of points is fully considered in this method [7, 38, and 43].

Changes in isotropy and anisotropy of variables are effective in window shape. The distance between the stations within the window from the center is used to calculate the weight of these stations. These weights are multiplied by the measured values of the stations. Finally, the center point of the window was estimated by the sum of these values.

The average of U values, $U_i(r)$, is calculated as follows [7, 13, and 18].

$$U_i(r) = \frac{\sum_{j=1}^{n_1} w_j(r)x_j - \mu}{\sigma} + \frac{\sum_{k=1}^{n_2} w_k(r)x_k - \mu}{\sigma} = \frac{\bar{x}_i(r) - \mu}{\sigma} \quad (1)$$

Where μ and σ are the mean and standard deviation, respectively. x_i and x_j are the measured values at stations j and k inside the window. $w_k(r)$ and $w_j(r)$ are the weights of these stations. is the weighted average of station i based on the surrounding stations' values. In this equation, j and k are related to samples with background and anomalous values, respectively. If the mean anomaly population is

DOI: https://doi.org/10.30564/jgr.v3i2.2935

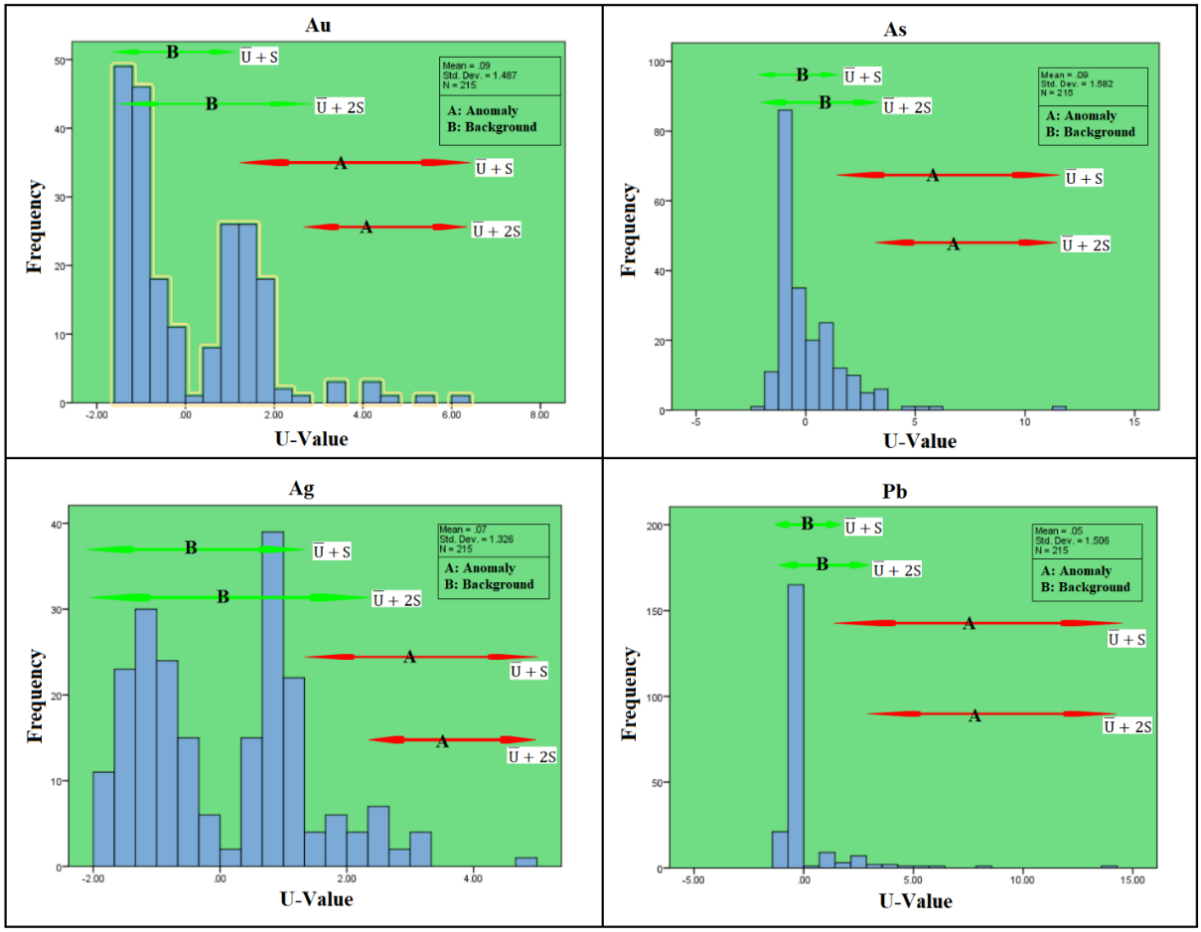

Figure 7. Histogram of U-Values for samples Au, As, Ag, and Pb.

μ_A and the mean background population is μ_B, then it will confirm the $\mu_A<\mu<\mu_B$.

A program was written in the Matlab software to implement the U-statistic algorithm on the study data. The program calculates the U-value for each point in the neighborhood of zero to 5000 meters (r_{max}) using the above equations and then assigns the highest value in absolute terms to the target point as U^*. These calculations were performed for the concentration of the gold element with 215 samples. The calculation starts from a circle with a radius of zero until 5000 m. For accuracy in calculating the distance between the two circles' radiuses in two sequential steps was considered 10 m, so 500 circles were drawn for each sampling point, and the U-value was calculated for each of them. The maximum of is determined for the point, and this value is stored as U^*. The histogram of the selected U values from U^* values for the elements of Au, As, Ag, and Pb is given in Figure 7. A minimum is seen at the zero points in this Figure. It is the boundary that passes out of the background and approaches the anomalous area and is approximately the boundary of the background and the anomaly values. The anomaly U values were separated according to the and criteria (Table 2). The number of anomalies samples separated by these criteria was presented in Table 3.

Table 2. The results of calculations of the U-spatial statistics method for the elements

Element	$\overline{U} + S$	$\overline{U} + 2S$
Au	1.57	3.06
As	1.67	3.25
Pb	1.55	3.06
Ag	1.39	2.72

 DOI: https://doi.org/10.30564/jgr.v3i2.2935

Table 3. The number of samples separated by U-spatial statistics method

$\overline{U}+S$												$\overline{U}+2S$			
Au				As			Ag			Pb		Au	As	Ag	Pb
8	79	88	135	13	22	95	8	163	172	78	87	212	22	16	81	85
22	80	89	136	14	48	111	12	164	173	79	88		46	17	85	86
46	81	90	142	15	55	178	47	165	174	80	89		47	55	86	87
47	82	91	143	16	56	179	81	166	175	81	90		85	56	168	88
51	83	92	212	17	57	180	83	167	176	82	91		93	57	169	89
56	84	93		18	58	181	84	168	177	83	92		94	58	170	90
58	85	94		19	61	182	85	169	187	84	93		95	180	171	91
62	86	95		20	93	184	86	170	188	85	94		136	181		92
78	87	127		21	94		132	171	189	86	95			184		

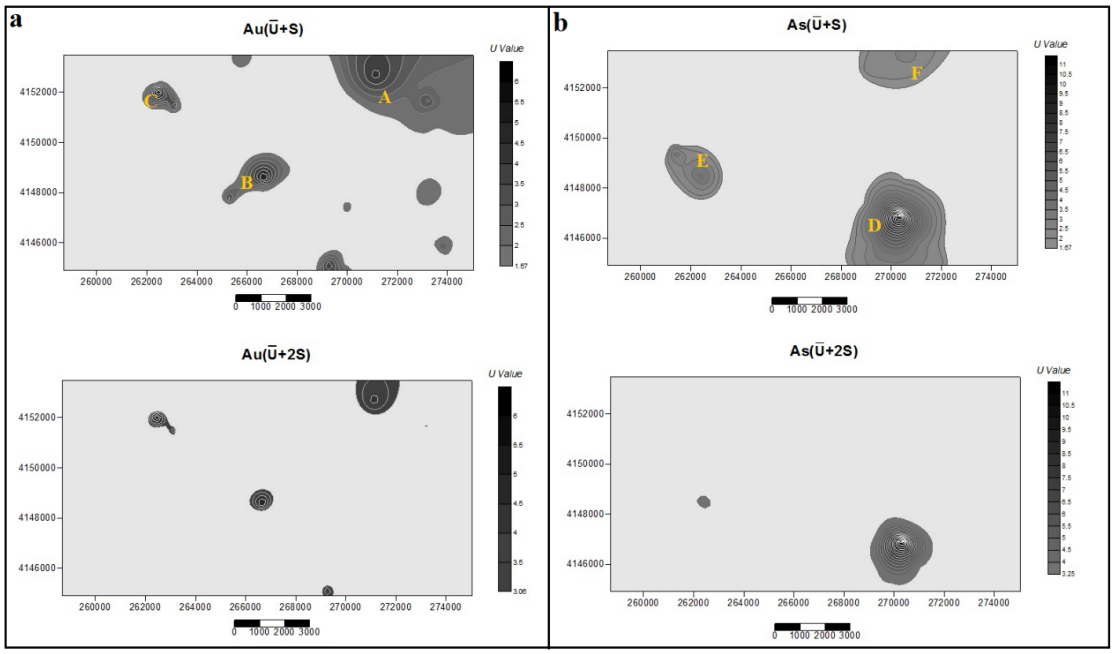

Figure 8. Anomalous areas map of Au (a) and As (b) elements obtained by the U-spatial statistics method.

Also, the anomalies areas map of the elements was obtained by these criteria are shown in Figure 8, 9. In these Figures, the gold anomalous zones are distinguished from the background zone with the pale gray color by the high color intensity of black. In these Figures, potential regions with higher anomaly intensities are shown in capital letters. In the Au element, the three limits A, B, and C are areas with significant haloes obtained by the criteria. The surface area of these haloes in the criteria is significantly reduced. The spatial dispersion of the other elements shows that As and Pb are in good agreement with the Au element in one of the anomalous areas (Figure 8, F zone,

DOI: https://doi.org/10.30564/jgr.v3i2.2935

and Figure 9, A zone). However, this overlap for the criteria is disappeared. Ag shows good overlap in one of the high concentration limits of Au (Figure 9, B zone), but this overlap disappears in other criteria of the U-spatial statistics method, too.

4.2 Classical Statistics (Mean Plus Values of Standard Deviation ())

In this method, the anomalous zones have been separated using the enrichment index data. First, the rock units were simplified by grouping them, and the number of the samples was obtained in these units by considering upstream of stream sediment samples. Then, by calculating the element enrichment index for all samples, data's distribution was investigated for the gold element, and the anomalous areas were determined.

4.2.1 Eliminating the Syngenetic Component

To eliminate or reduce the effect of lithology on the data, it is necessary to classify the samples according to the effective rock populations. In the regional surveys of the stream sediments, effective rock units in the syngenetic component are located upstream of the sample in the catchment basin [26].

Therefore, the sampling plan was first fitted to the geological map. Then, by determining the catchment basin of each sample (upstream of the sample), all rock units were identified whose sediments resulted from their erosion contributed to the formation of the sample. After separating statistical populations, the effect of lithology in each population was eliminated by normalizing the values to the median. Finally, the populations were mixed again and studied under a homogeneous population. Figure 10 shows the location of the sampling on the rock units and streams of the area.

4.2.2 Classification of Samples by the Type and Number of Upstream Rocks

To reducing the number of statistical populations, similar rock outcrops were combined and considered as a rock population. Abbreviations and upstream rock types were summarized in Table 4 based on the 1:20000 geological map. The following is a classification of samples by the number of upstream rock types:

A - single-rock sub-population: 84 samples (including seven different rock types)

B - Two-rocks sub-population: 69 samples (including thirteen types of two-rock groups)

C - Three-rocks sub-population: 36 samples (including eleven types of three-rock groups)

D - Sub-population of more than three-rocks: 26 samples

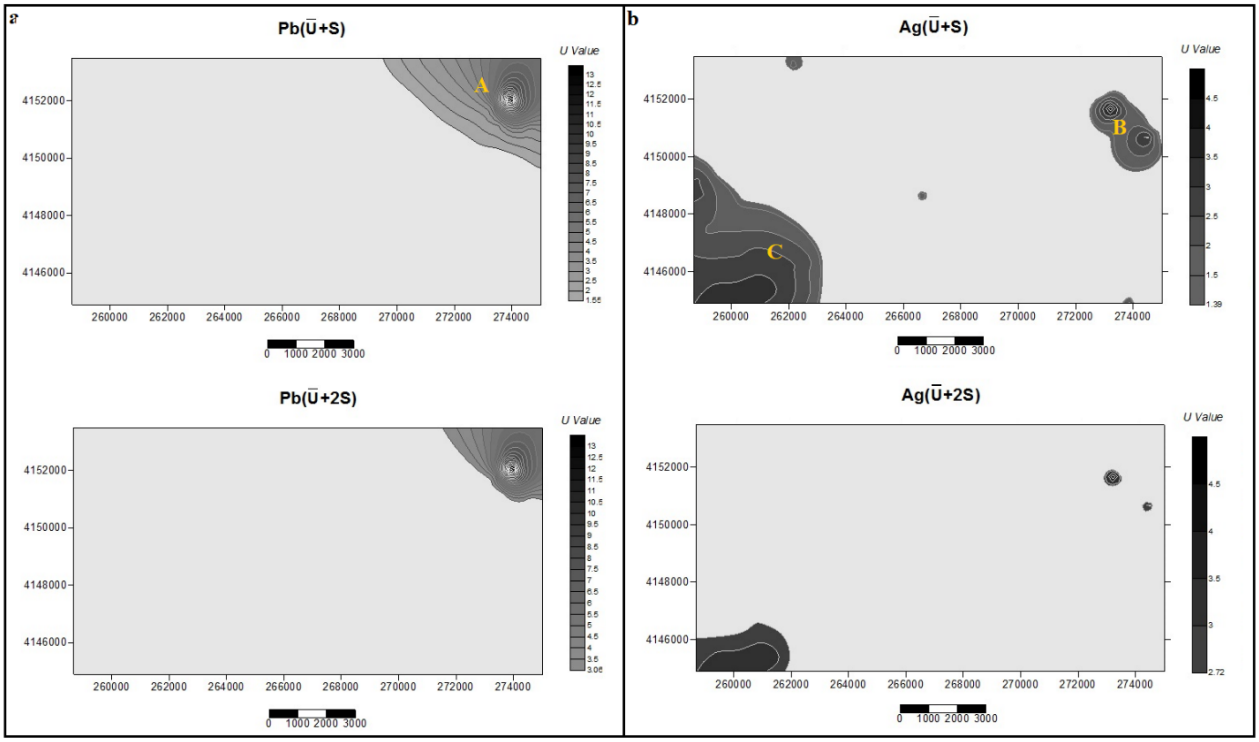

Figure 9. Anomalous areas map of Pb (a) and Ag (b) elements obtained by the U-spatial statistics method.

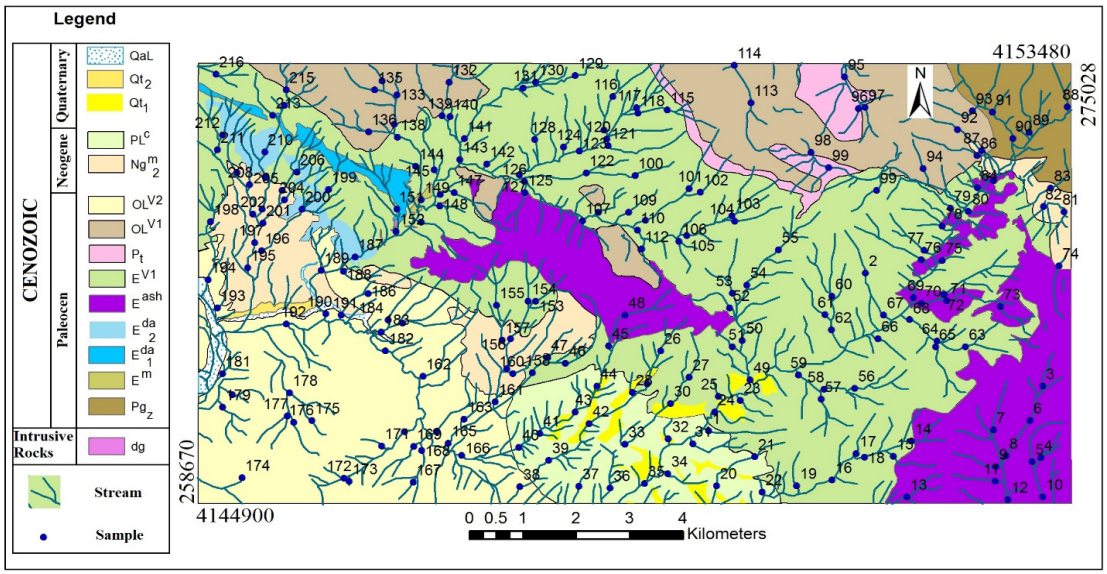

Figure 10. Location of the samples on the rock units and the streams of the Khoshnameh area.

Table 4. Summarization of upstream rock types of the stream sediments samples in Khoshnameh map of 1:20000

Rock population	Description	Related rock units
OL	Igneous rocks: trachybasalt to brown trachyandesite, rhyolite, rhyodacite	OLv2, OLv1
Ng	Red sandstone, siltstone and marl	Ng2m
PQ	Sedimentary rocks: conglomerate, sandstone, alluvial-diluvial deposits, spray limestone, Acid pyroclastics	PLc, Qt1, Qal, Pgz, Pt
Vol	Volcanic rocks: Andesite to dacite, basic volcanic rocks, pumicite	Ev1, Eda2،Eda1, Em, Eash

For each of the above populations with more than ten samples, statistical parameters were calculated to obtain the element enrichment coefficient. This coefficient was calculated using dividing the values of each particular element in a population by its median value. The rest of the population, where the sample size has not reached the quota (10 samples) for statistical computation, is mixed in a population and then subjected to cluster analysis. After cluster analysis on these samples, two groups were determined for these data.

Statistical calculations were performed on these two populations, and a homogeneous population was established as an enrichment index. The median of each rock population is calculated. Table 5 shows rock populations and their median. In this Table, upstream rocks include two groups of single-rock, three groups of two-rocks, and three groups of three-rocks, in which there are more than ten samples for each group. The statistical parameters were calculated for these groups.

Table 5. Values of elements frequency median as functional from upstream rock populations

Rock population	Au (ppb)	As (ppm)	Ag (ppm)	Pb (ppm)
OL	0.5	6.6	0.83	11
Vol	1	8	0.54	7.6
Vol, OL	0.5	8.8	0.63	12.1
Vol, PQ	0.5	8.8	0.24	7.35
Vol, Ng	0.5	9	0.65	10.05
PQ, Vol, OL	1	9	0.4	9.4
Vol, Ng, OL	0.5	9	0.65	10.2
PQ, Vol, Ng	1	8.4	0.58	10.5

DOI: https://doi.org/10.30564/jgr.v3i2.2935

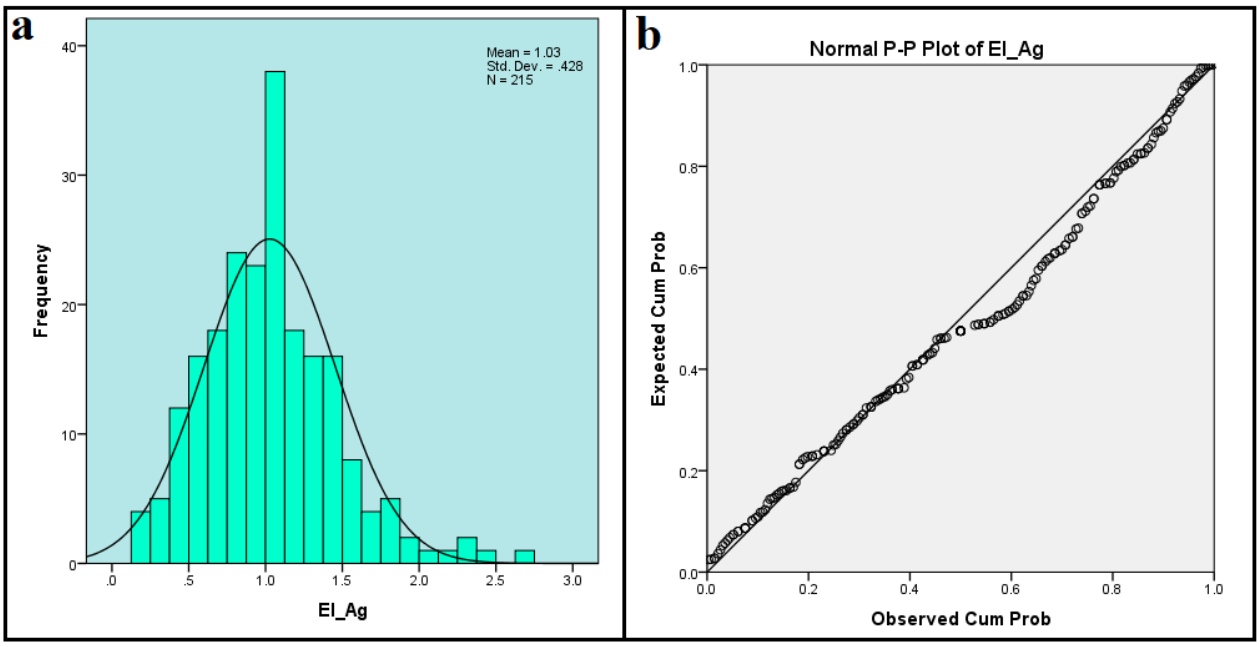

Figure 11. Frequency distribution of Ag element: a) Frequency histogram of Ag element data, which shows a normal distribution for this element. b) P-P plot of data that confirms a normal distribution of the Ag element.

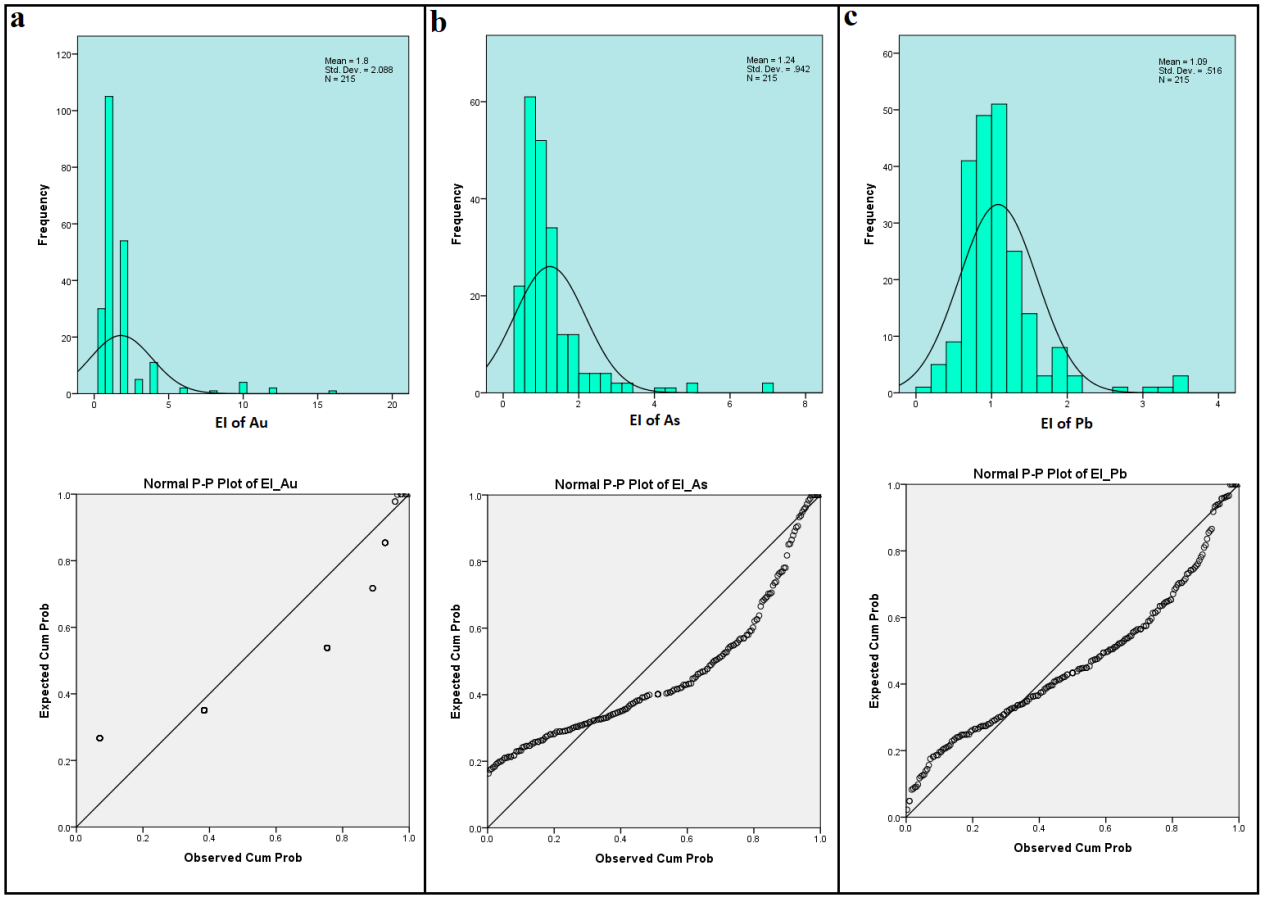

Figure 12. Frequency distribution of Au (a), As (b), and Pb (c) elements. Histogram diagram of the element shows a skewness to the left, and P-P plots confirm a log-normal distribution for the elements.

 DOI: https://doi.org/10.30564/jgr.v3i2.2935

4.2.3 Frequency Distribution of Data

It is essential to determine the frequency distribution of data in identifying the background from anomaly using the method. A normal distribution is one of the most common statistical distributions. In exploring the nature of mineral data distribution, including exploration and extraction, the normal distribution has particular importance. The history of using a normal distribution for exploration data is very long. The reason is the absence of another comprehensive distribution and the unique characteristics of this particular distribution. Often, exploration data can be assumed to be normal with an appropriate conversion.

In many cases, the exploration data has an asymmetric distribution with a positive skew. This means that samples with smaller values (e.g., low concentration) are more abundant, and samples with larger values (e.g., high concentration) are scarce. Under these conditions, by converting the data under the logarithmic function, the converted distribution is symmetric and approaches the normal distribution. The distribution of these data is called log-normal.

After identifying outlier values using the Q-Q Plot and correcting these values, the data distribution diagram and P-P plot for each element were plotted. Figure 11 shows the Ag element's frequency distribution using the Histogram and P-P plot of this element data. The frequency histogram shows a normal distribution, and the P-P plot of data confirms this distribution for the Ag element. According to these graphs, the distribution of the Au, As, and Pb elements were detected log-normal.

The logarithm of the data was calculated, and then the histograms and their P-P plots were plotted. The histogram diagram and P-P plot of these elements as a log-normal distribution are shown in Figure 12 and 13.

4.2.4 Separation of the Anomaly from the Background

In the exploration surveys, the data distribution is often log-normal due to high skewness. In these surveys, often, large amounts of the distribution function constitute anomalous populations. These values, which are separable from other data (background values), are potential zones

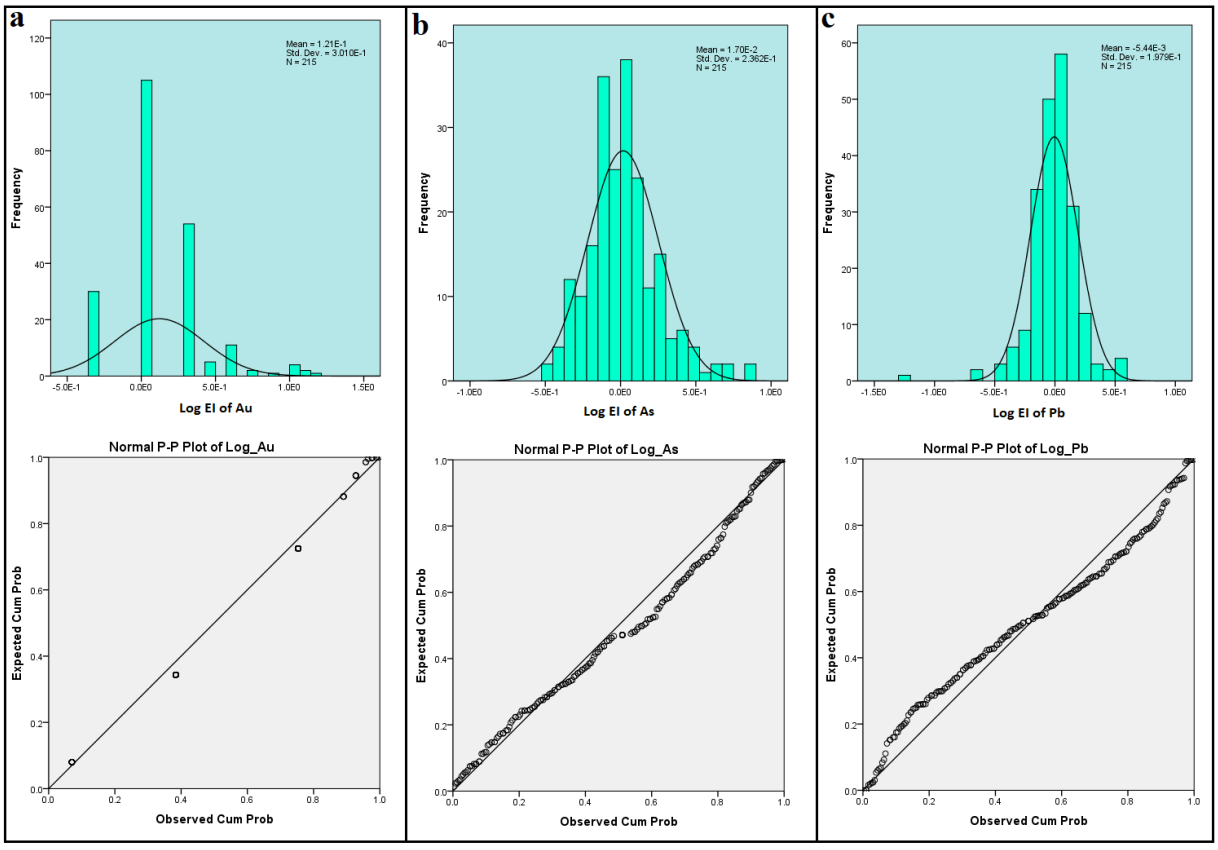

Figure 13. Frequency distribution of the logarithm of Au (a), As (b), and Pb (c) elements data. Histogram diagram of the logarithm of the element shows a symmetrical graph, and P-P plots confirm a normal distribution for the logarithm of the elements.

DOI: https://doi.org/10.30564/jgr.v3i2.2935

for economic mineralization.

To separate the anomaly values from the background, frequency graphs of the geochemical values were considered and used. Also, the mean plus values of the standard deviation () method is an efficient and simple method for separating the anomalies from the background. In this method, it must first calculate the mean values and standard deviation of the data.

The mean of the data is used to determine the amount of geochemical background. Because boundary values affect the mean of the data, these values must first be identified and separated from the other data. Then the arithmetic mean of the remaining data calculated as the background value. Data frequency histogram can extract boundary values [44, 45, and 46].

The best way to calculate the background data's standard deviation is to use the method of separating the background data from the anomalous data. So, first, the values of the separation limit of positive and negative anomalies from the background should be determined according to the frequency histogram of the data. Then the standard deviation of the data should be calculated in the range [46].

In this method, if the data distribution is normal, by determining the background (C_{bg}) can calculate the anomaly threshold at three confidence levels of possible ($C_{an.1}$), probable ($C_{an.2}$), and definitive ($C_{an.3}$) using the following equation:

$$C_{an}=C_{bg}+ns \quad (2)$$

Where s is the standard deviation, and n is a coefficient, which can be values of 1,2 and 3. If the value of n is higher, the anomaly areas become smaller. So, the cost of exploration is lower, but at the same time, it is possible to eliminate some probable anomalies.

If the distribution of data is log-normal, the anomaly threshold values are calculated as follows:

$$C_{an}=C_{bg}\times\varepsilon^{t} \quad (3)$$

Where t is a value of 1, 2, or 3, and ε is antilog (S_{log}) [28].

Background and anomaly values for the elements were

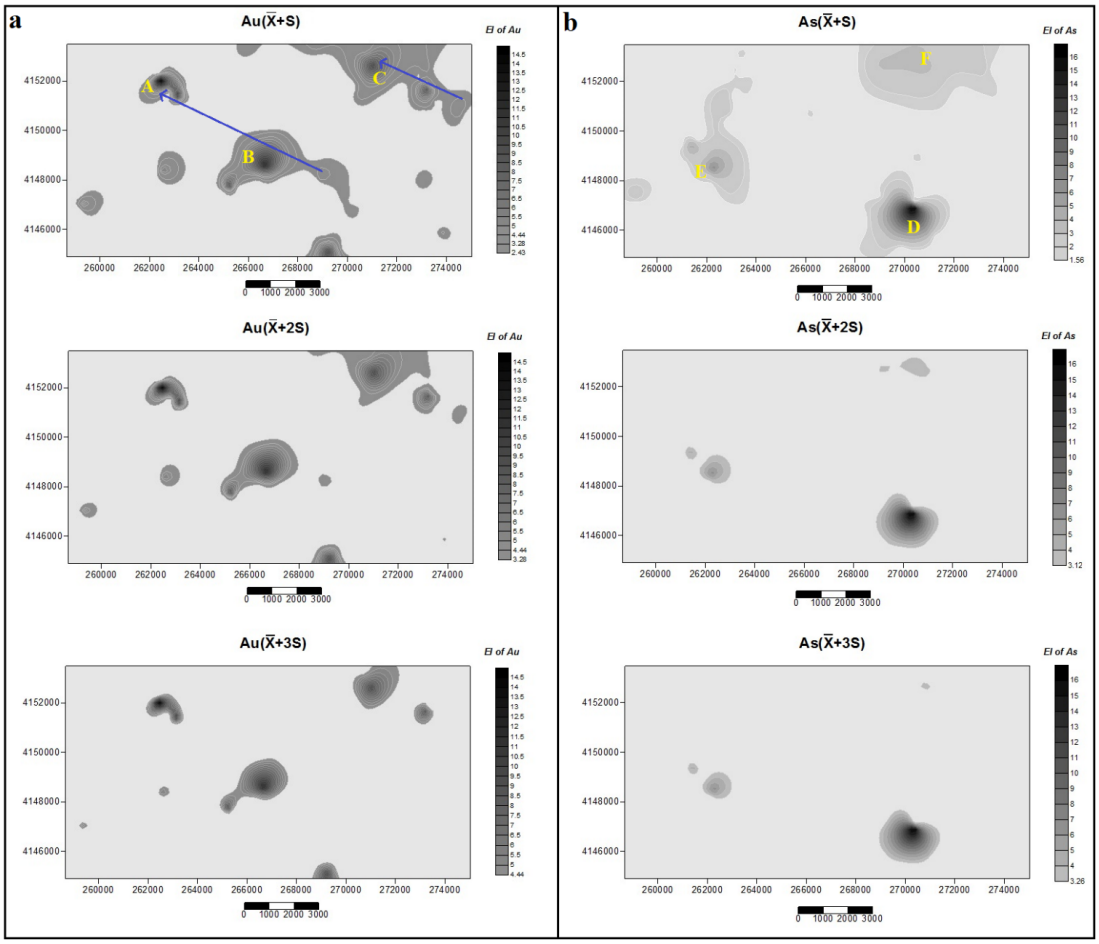

Figure 14. Anomalous areas map of Au (a) and As (b) elements obtained by method

 DOI: https://doi.org/10.30564/jgr.v3i2.2935

calculated by performing the necessary calculations (Table 6). According to these values, the geochemical map of the elements was plotted in which the anomalous regions were determined. It is also possible to identify how the elements are distributed and how they relate to each other.

Table 6. Values of the background and anomaly thresholds for the elements by the method

Element	Distribution	Background	Can.1	Can.2	Can.3
Au	Log-normal	1.8	2.43	3.28	5.45
As	Log-normal	1.24	1.56	3.12	3.26
Ag	Normal	1.03	1.45	1.88	2.3
Pb	Log-normal	1.09	1.32	1.61	1.96

Figure 14 and 15 show the results of the method for the Au, As, Pb, and Ag elements. These results, which are dispersion maps of geochemical anomalies, also show the relationship of elements dispersion to each other. Figure 14a shows the geochemical map of the gold anomaly areas. The primary trend for the potential areas is approximately the SE-NW, which is indicated by the arrow on the map (Figure 14a). It is well overlapped with the general trend of the study area occurrences (Figure 3(b)). Among the gold-related elements, the sizeable anomalous zone of Pb and As with different concentration intensities (Figure 14b, D, E, and F limits and Figure 15a, A, B, and C limits) overlap well with the gold anomalous areas. This shows a close relationship between Pb and As with the Au element, especially in the X+S criteria, and also confirms the close dependency identified by the dendrogram. The Ag anomalies show a normal dispersion in the area that did not react much in the expansion limit of high concentra-

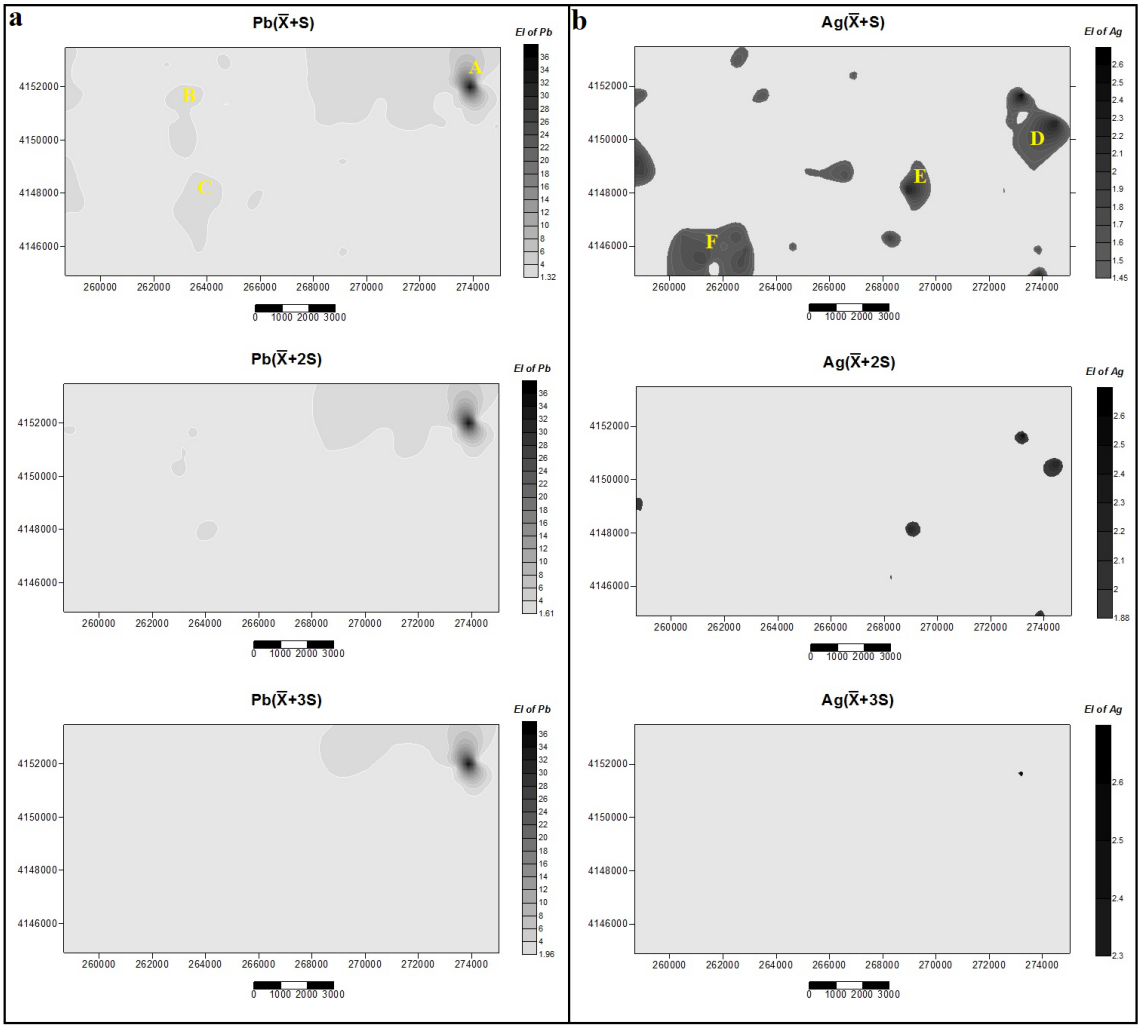

Figure 15. Anomalous areas map of Pb (a) and Ag (b) elements obtained by method

DOI: https://doi.org/10.30564/jgr.v3i2.2935

tions of gold. What can be discussed here is the status of the current erosion level or the relatively low relationship of this element with mineralization.

5. Comparison of the Methods

Comparison of the methods was made considering the position of discovered occurrences and the occurrences obtained from these methods, the flexibility of the methods in separating the anomalous zones, and the two-dimensional spatial correlation of the three elements As, Pb, and Ag with Au element. In order to better compare the methods, the contour map obtained from the U-spatial statistics (two maps) and (three maps) methods were considered (Figure 16). To compare the calculated models with the observed model, the position of the occurrences is also fitted on the final maps. These occurrences have already been identified by the Ardabil province SAMT organization. To avoid overcrowding of the map and a more exact comparison, other parameters in the region, such as rock units, were avoided. There are two occurrences related to gold mineralization in the region. These occurrences are fitted to the anomalous areas obtained by different methods. Based on the available information from the study area's known occurrences, the threshold calculated from both criteria of the U-statistical and confirms both occurrences.

Studies of the haloes show that the haloes obtained from the criteria are very close to the haloes obtained by the criteria in term of extent. There is a good agreement with the detected occurrences. The haloes obtained by the method have considerable flexibility. The areas within the anomaly boundary have been recorded by this method. It has in good agreement with the occurrences in the area. The reason for this flexibility is probably due to data of the elemental enrichment index in this method that has affected the creation of clearer mineralization. Because of in calculating this parameter, the impact of upstream geological units for any sample was considered in stream

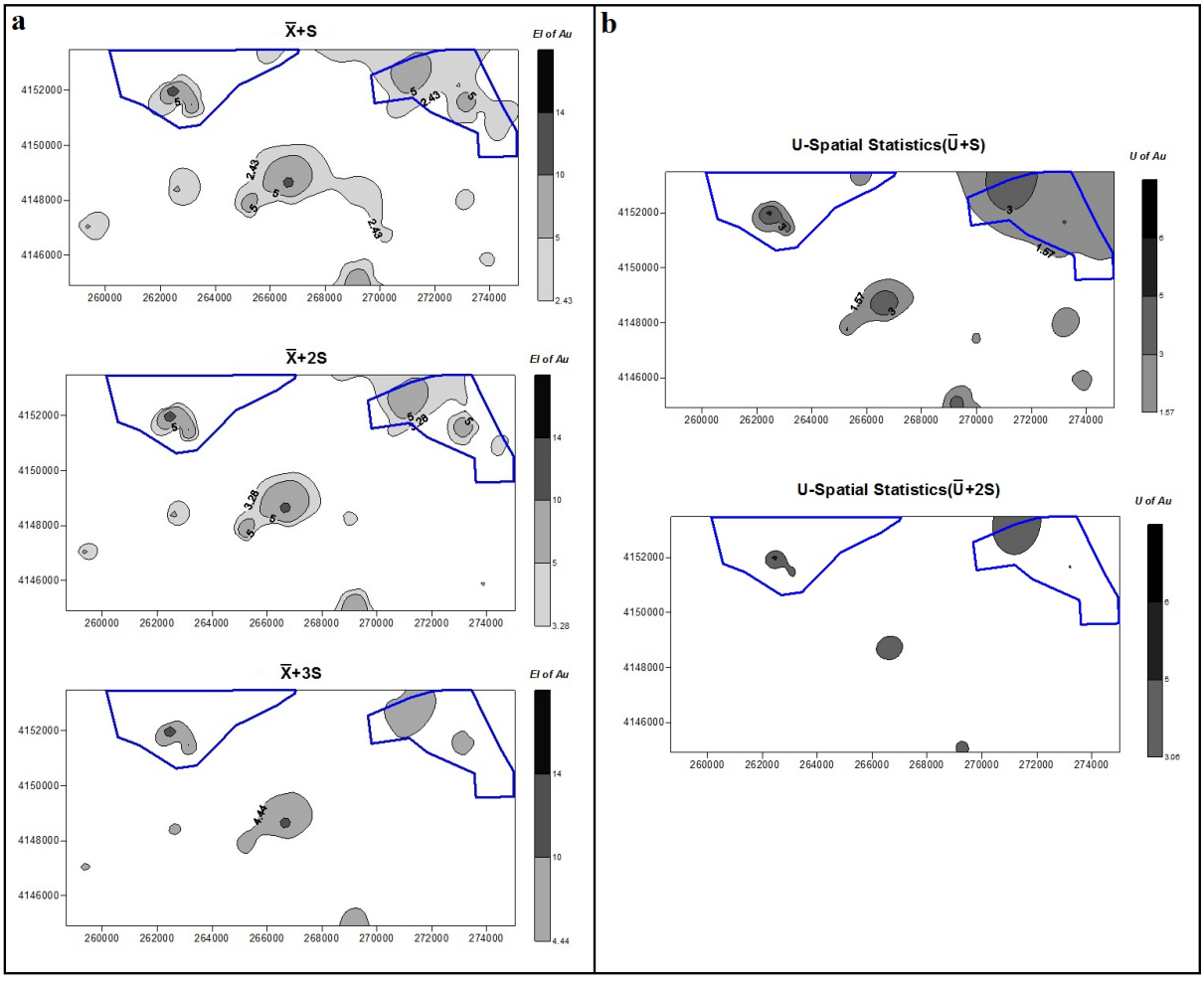

Figure 16. Contour map of anomalous areas: a: method, b: method

Distributed under creative commons license 4.0 DOI: https://doi.org/10.30564/jgr.v3i2.2935

sediments. In the northeast of the area, criteria shows wider haloes than criteria. By changing the threshold value to twice the standard deviation, the haloes obtained by the U-statistic method significantly loses its extent, but retains its extent concerning the discovered occurrences. Another point to note is that both methods show another anomaly in the center of the area.

This anomaly is not found among the occurrences. Given that both methods confirm this zone, so it is notable for continuing exploration operations. The results of the two methods in presenting the maps of mineralization zones and comparing these dispersions with the correlation of the elements in the dendrogram show that the relationship between the elements' correlation and their surface dispersion with each other which is one of the geochemical characterizations of each type of deposit, is better and more clearly expressed by criteria.

6. Conclusions

There are various methods for separating geochemical anomalies from the background, and the efficiency of these methods is an important issue in the field. U-spatial statistics and are two robust methods for separating geochemical anomalous zones. The study area is located in the Khashtnameh district of Hashtjin, in Ardabil province. In this area, gold mineralization is of epithermal type. The results show that there is a close relationship between U-spatial statistics and methods. This is more evident for the gold element in the northeast of the area. The two-dimensional spatial distribution of the elements and their relationship with each other using the criteria was represented better and more realistic than other methods. Of course, the presence of a regular network seems to affect the sensitivity of the U-statistics results.

In this research, two methods' results were compared with each other in detecting gold haloes. Given that the U-spatial statistical method is more sensitive in considering the spatial location of the samples and the method has more sensitive in separating anomalous populations compared to the mentioned method, it seems that in analyzing the stream sediment data and separating anomaly from the background are a reasonable proposition. Among these methods, it seems that criteria in the method have the most optimal halo extent and be the more appropriate criteria for epithermal type deposits compared to other criteria in separating anomalous zones.

Acknowledgement

The authors thank the Industry, Mine & Trade Organization of Ardabil province in Iran for providing the data.

References

[1] Sinclair, A., (1974), Selection of threshold values in geochemical data using probability graphs. Journal of Geochemical Exploration, 3: 129-149.

[2] Levinson, A.A., (1974), Introduction to exploration geochemistry. Applied publishing Ltd, Illinois, USA, pp. 924.

[3] Govett, G., Goodfellow, W., Chapman, R. and Chork, C., (1975), Exploration geochemistry—distribution of elements and recognition of anomalies. Journal of the International Association for Mathematical Geology, 7: 415-446.

[4] Sinclair, A., (1991), A fundamental approach to threshold estimation in exploration geochemistry: probability plots revisited. Journal of Geochemical Exploration, 41: 1-22.

[5] Cheng, Q., Agterberg, F. and Ballantyne, S., (1994), The separation of geochemical anomalies from background by fractal methods. Journal of Geochemical exploration, 51: 109-130.

[6] Yusta, I., Velasco, F. and Herrero, J.-M., (1998), Anomaly threshold estimation and data normalization using EDA statistics: application to lithogeochemical exploration in Lower Cretaceous Zn–Pb carbonate-hosted deposits, northern Spain. Applied geochemistry, 13: 421-439.

[7] Cheng, Q., (1999), Spatial and scaling modelling for geochemical anomaly separation. Journal of Geochemical exploration, 65: 175-194.

[8] Cheng, Q., Xu, Y. and Grunsky, E., (2000), Integrated spatial and spectrum method for geochemical anomaly separation. Natural Resources Research, 9: 43-52.

[9] Gonçalves, M.A.,, Mateus, A. and Oliveira, V., (2001), Geochemical anomaly separation by multifractal modelling. Journal of Geochemical Exploration, 72: 91-114.

[10] Li, C., Ma, T. and Shi, J., (2003), Application of a fractal method relating concentrations and distances for separation of geochemical anomalies from background. Journal of Geochemical exploration, 77: 167-175.

[11] Lima, A., De Vivo, B., Cicchella, D., Cortini, M. and Albanese, S., (2003), Multifractal IDW interpolation and fractal filtering method in environmental studies: an application on regional stream sediments of (Italy), Campania region. Applied geochemistry, 18: 1853-1865.

[12] Zuo, R., Cheng, Q. and Xia, Q., (2009), Application of fractal models to characterization of vertical distribution of geochemical element concentration. Journal

  DOI: https://doi.org/10.30564/jgr.v3i2.2935

of Geochemical Exploration, 102: 37-43.

[13] Ghavami-Riabi, R., Seyedrahimi-Niaraq, M., Khalokakaie, R. and Hazareh, M., (2010), U-spatial statistic data modeled on a probability diagram for investigation of mineralization phases and exploration of shear zone gold deposits. Journal of Geochemical exploration, 104: 27-33.

[14] Ghannadpour, S.S. and Hezarkhani, A., (2016), Introducing 3D U-statistic method for separating anomaly from background in exploration geochemical data with associated software development. Journal of Earth System Science, 125: 387-401.

[15] Ghezelbash, R. and Maghsoudi, A., (2018), Comparison of U-spatial statistics and C–A fractal models for delineating anomaly patterns of porphyry-type Cu geochemical signatures in the Varzaghan district, NW Iran. Comptes Rendus Geoscience, 350: 180-191.

[16] Liu, Y., Cheng, Q., Carranza, E.J.M. and Zhou, K., (2019), Assessment of geochemical anomaly uncertainty through geostatistical simulation and singularity analysis. Natural Resources Research, 28: 199-212.

[17] Yousefi, M., Kreuzer, O.P., Nykänen, V. and Hronsky, J.M., (2019), Exploration information systems-a proposal for the future use of GIS in mineral exploration targeting. Ore Geology Reviews: 103005.

[18] Seyedrahimi-Niaraq, M., Hekmatnejad, A., (2021), The efficiency and accuracy of probability diagram, spatial statistic and fractal methods in the identification of shear zone gold mineralization: a case study of the Saqqez gold ore district, NW Iran. Acta Geochimica, https://doi.org/10.1007/s11631-020-00413-7.

[19] Rose, A.W., Hawkes, H.E. and Webb, J.S., (1979), Geochemistry in mineral Exploration. Academic Press, London, pp.657.

[20] Cheng, Q., (2001), Multifractal and geostatistic methods for characterizing local structure and singularity properties of exploration geochemical anomalies. Journal of China University of Geosciences, 26:161-166.

[21] Carranza, E.J.M., (2008), Geochemical anomaly and mineral prospectivity mapping in GIS. Vol 11, Elsevier.

[22] Darabi-Golestan, F., Ghavami-Riabi, R., Khalokakaie, R., Asadi-Haroni, H. and Seyedrahimi-Niaraq, M., (2013), Interpretation of lithogeochemical and geophysical data to identify the buried mineralized area in Cu-Au porphyry of Dalli-Northern Hill. Arabian Journal of Geosciences, 6: 4499-4509.

[23] Shahi, H., Ghavami, R., Kamkar Rouhani, A., Asadi-Haroni, H., (2015), Application of Fourier and wavelet approaches for identification of geochemical anomalies. Journal of African Earth Sciences, 106:118-128.

[24] Parsa, M., Maghsoudi, A., Yousefi, M. and Sadeghi, M., (2017), Multifractal analysis of stream sediment geochemical data: Implications for hydrothermal nickel prospection in an arid terrain, eastern Iran. Journal of Geochemical Exploration, 181: 305-317.

[25] Mahdiyanfar, H., (2019). Detection of Mo geochemical anomaly in depth using a new scenario based on spectrum–area fractal analysis. Journal of Mining and Environment, 10(3), pp.695-704.

[26] Wellmer, F.W., (1998), Statistical Evaluations in Exploration for Mineral Deposits. Springer New York, pp.379.

[27] Mandelbrot, B.B.,, Pignoni, R., (1983), The fractal geometry of nature, WH freeman, New York. vol 173.

[28] Solovov, A.P., (1985), Geochemical prospecting for mineral deposits. Mir Publisher.

[29] Stanley, C.R. and Sinclair, A.J., (1989), Comparison of Probability Plots and the Gap statistic in selection of Threshold of Exploration Geochemistry Data. Journal of Geochemical Exploration. 32:355-357.

[30] Agterberg, F.P., Cheng, Q., Brown, A. and Good, D., (1996), Multifractal modeling of fractures in the Lac du Bonnet batholith, Manitoba. Computers & Geosciences, 22:497-507.

[31] Rantitsch, G., (2004), Geochemical exploration in a mountainous area by statistical modeling of polypopulational data distributions. Journal of Geochemical Exploration, 82: 79-95.

[32] Cheng, Q., Xia, Q., Li, W., Zhang, S., Chen, Z., Zuo, R. and Wang, W., (2010), Density/area power-law-models for separating multi-scale anomalies of ore and toxic elements in stream sediments in Gejiu mineral district, Yunnan Province, China. Biogeosciences, 7:3019–3025.

[33] Afzal, P., Alghalandis, Y.F., Khakzad, A., Moarefvand, P., Omran, N.R., (2011), Delineation of mineralization zones in porphyry Cu deposits by fractal concentration–volume modeling. Journal of Geochemical exploration, 108: 220-232.

[34] Yousefi, M. and Carranza, E.J.M., (2015), Prediction–area (P–A) plot and C–A fractal analysis to classify and evaluate evidential maps for mineral prospectivity modeling. Computers & Geosciences, 79: 69-81.

[35] Zuo, R., (2017). Machine learning of mineralization-related geochemical anomalies: A review of potential methods. Natural Resources Research, 26(4), pp.457-464.

[36] Wang, Z., Zuo, R. and Dong, Y., (2019). Mapping

 DOI: https://doi.org/10.30564/jgr.v3i2.2935

geochemical anomalies through integrating random forest and metric learning methods. Natural Resources Research, 28(4), pp.1285-1298.

[37] Grunsky, E.C. and de Caritat, P., (2020). State-of-the-art analysis of geochemical data for mineral exploration. Geochemistry: Exploration, Environment, Analysis, 20(2), pp.217-232.

[38] Cheng, Q., Agterberg, F. and Bonham-Carter, G., (1996), A spatial analysis method for geochemical anomaly separation. Journal of Geochemical exploration, 56: 183-195.

[39] Geology society of Iran (GSI), (2006), Report of gold exploration condition in Iran.

[40] Zarnab Ekteshaf Company (ZE Co.), (2006), Exploration of polymetallic elements (Gold and other elements) in the Khoshnameh village limit of Hashtjin. Report of Ardabil province SAMT organization.

[41] Towsehe Olume Zamin Company (TOZ Co.), (2003), Systematic geochemical explorations in leaf of Hashtjin (1:100,000). Report of Ardabil province SAMT organization.

[42] Stanford, F., Pierson, T. and Crovelli, R.A., (1993), An objective replacement method for censord geochemical data. Mathematical Geology, 27(1):59-79.

[43] Lin, Y.P., (2002), Multivariate geostatistical methods to identify and map spatial variations of soil heavy metals. Environmental Geolology, 42:1-10.

[44] Hawkes, H.E. and Webb, J.S., (1962), Geochemistry in mineral exploration harper and row, New York, P.415.

[45] Lepeltier, C., (1969), A simplified statistical treatment of geochemical data by ghraphical representation. Economic Geology, 64:538-550.

[46] Solovov, A.P., (1990), Handbook on Geochemical Prospecting for Useful Minerals, Moscow. Nedra Publishing house.

DOI: https://doi.org/10.30564/jgr.v3i2.2935